Electron- and hole-doping effects on the electronic structure of manganite studied by x-ray absorption spectroscopy

2004 J. Phys.: Condens. Matter 16 3791

(http://iopscience.iop.org/0953-8984/16/21/027)

INSTITUTE OF PHYSICS PUBLISHING JOURNAL OF PHYSICS: CONDENSED MATTER

J. Phys.: Condens. Matter **16** (2004) 3791–3799 PII: S0953-8984(04)69719-0

Electron- and hole-doping effects on the electronic structure of manganite studied by x-ray absorption spectroscopy

K Asokan[1,5], J C Jan[1], K V R Rao[1,6], J W Chiou[1], H M Tsai[1], S Mookerjee[1,5], W F Pong[1], M-H Tsai[2], Ravi Kumar[3], Shahid Husain[4] and J P Srivastava[4]

[1] Department of Physics, Tamkang University, Tamsui 251, Taiwan
[2] Department of Physics, National Sun Yat-Sen University, Kaohsiung 804, Taiwan
[3] Nuclear Science Centre, Aruna Asaf Ali Marg, New Delhi-110 067, India
[4] Department of Physics, Aligarh Muslim University, Aligarh-202002, India

Received 27 September 2003, in final form 31 March 2004
Published 14 May 2004
Online at stacks.iop.org/JPhysCM/16/3791
DOI: 10.1088/0953-8984/16/21/027

Abstract

The electronic structures of hole-doped $La_{0.7}Ca_{0.3}MnO_3$ and electron-doped $La_{0.7}Ce_{0.3}MnO_3$ manganites are investigated by x-ray absorption near-edge structure spectroscopy at the O and Mn K-, and Mn $L_{3,2}$-edges. The Mn K- and $L_{3,2}$-edge results show that Ce dopants increase the occupation of the Mn 4p and majority-spin e_g orbitals and reduce the positive effective charge of some Mn ions. However, Ce doping also induces holes in O 2p derived states. As for $La_{0.7}Ca_{0.3}MnO_3$, in contrast to previous understanding that Ca doping converts some Mn ions into the Mn^{4+} state, we find that Ca dopants actually increase the number of majority-spin e_g electrons. We find instead that the holes created by Ca dopants are in the O 2p derived states.

1. Introduction

Rare-earth manganites show extraordinary phase transitions and various anomalous properties such as colossal magnetoresistance (CMR), charge ordering, and anomalous magnetization [1]. The fundamental origin of such anomalous properties remains a puzzle. However, the interplay between spin, orbital, and charge degrees of freedom has been found to be crucial, and the double exchange (DE) model has usually been used for a basic understanding of these properties [1–4]. Extensive investigations have been performed for the $La_{1-x}Ca_xMnO_3$ compounds, which are called hole-doped manganites because the Ca ions generate holes in

[5] On leave from: Nuclear Science Centre, Aruna Asaf Ali Marg, New Delhi-110 067, India.
[6] Permanent address: Department of Physics, University of Rajasthan, Jaipur 302004, India.

$LaMnO_3$ (hereafter referred to as LM) [1, 3]. In contrast, Ce-doped LM, i.e. $La_{1-x}Ce_xMnO_3$, are called electron-doped manganites because the Ce ions donate electrons [5–7]. The DE model was not satisfactory for explaining metal–insulator and ferromagnetic transitions, and the concomitant CMR phenomenon in the manganites [1–4]. X-ray absorption near-edge structure (XANES) spectroscopy is a sensitive probe for the electronic properties, which can provide information about the valency, the unoccupied electronic states, and the effective charge of the absorber atom in a solid [8]. Asokan *et al* [9] and Mitra *et al* [10], based on an XANES study mainly at Mn $L_{3,2}$- and Ce $M_{5,4}$-edges, found electron doping in Ce-doped LM. In this study, we have performed XANES measurements at the O and Mn K-, and Mn $L_{3,2}$-edges to understand the effects of hole (Ca) and electron (Ce) doping on the electronic property of the manganites, especially the charge state of the Mn ions. However, much emphasis is placed on the compositions, $La_{0.7}Ca_{0.3}MnO_3$ (Ca-LM) and $La_{0.7}Ce_{0.3}MnO_3$ (Ce-LM), which represent hole- and electron-doped manganites, respectively.

2. Experimental details

All the Ca- and Ce-doped manganites were made from respective stoichiometric mixtures of La_2O_3, $CaCO_3$, $MnCO_3$, and La_2O_3, CeO_2, Mn_2O_3 by the ceramic method. For Ca-doped manganites, the mixture was initially heated at 950 °C for decarbonation and then at 1000 °C in air for 72 h with intermediate grindings. The resulting powder was pressed into pellets and sintered at a sufficiently high temperature (1300 °C) to ensure maximum compositional homogeneity. On the other hand, Ce-doped manganites were initially heated at 1200 °C for a few days with intermediate grindings. Finally, the powder was pressed into pellets and sintered in air at above 1300 °C for a few days and then cooled to room temperature. These samples were characterized by x-ray diffraction and magnetoresistivity measurements. These are detailed in [11]. All these samples were free from impurity phases. The Ca-LM and Ce-LM samples have magnetic transition (Curie) temperatures of 245 and 274 K and orthorhombic structures with lattice parameters of $a = 5.51$ Å, $b = 5.49$ Å and $c = 7.80$ Å and $a = 5.47$ Å, $b = 5.42$ Å, and $c = 7.67$ Å, respectively [9, 11]. XANES measurements at the O K- and Mn $L_{3,2}$-edges were carried out using the high-energy spherical grating monochromator (HSGM) beamline at the Synchrotron Radiation Research Center (SRRC), Hsinchu, Taiwan, operating at 1.5 GeV with a maximum stored current of 200 mA. The spectra were obtained using the sample drain current mode at room temperature, and the vacuum in the experimental chamber was in the low range of 10^{-9} Torr. The typical resolution of the HSGM beamline was better than ∼0.2 eV. The wiggler beamline BL17C of SRRC was also used for the XANES measurements at the Mn K-edge in the fluorescence mode, and the resolution was about 0.5 eV. It may be noted that the energy positions of Ce L_1 (6548 eV) and Mn K-edges (6539 eV) are very close. However, the edge jump and fluorescence yield for the Mn K-edge is significantly higher than for the Ce L_1-edge, and hence there was no interference of these edges in the spectra.

3. Results and discussion

For manganites the electronic structure close to the Fermi level (E_F) is dominated by Mn 3d and O 2p states [1–3, 12]. Figure 1 shows the normalized spectra at the O K-edges of some of the Ca- and Ce-doped manganites with various compositions. All spectra were normalized in the energy range between 550 and 560 eV (not fully shown in the figure) after subtracting the background. The main effects of these substitutions are to vary the electronic structure of 3d derived band and to alter the interatomic distances and bond angles. Four main features in

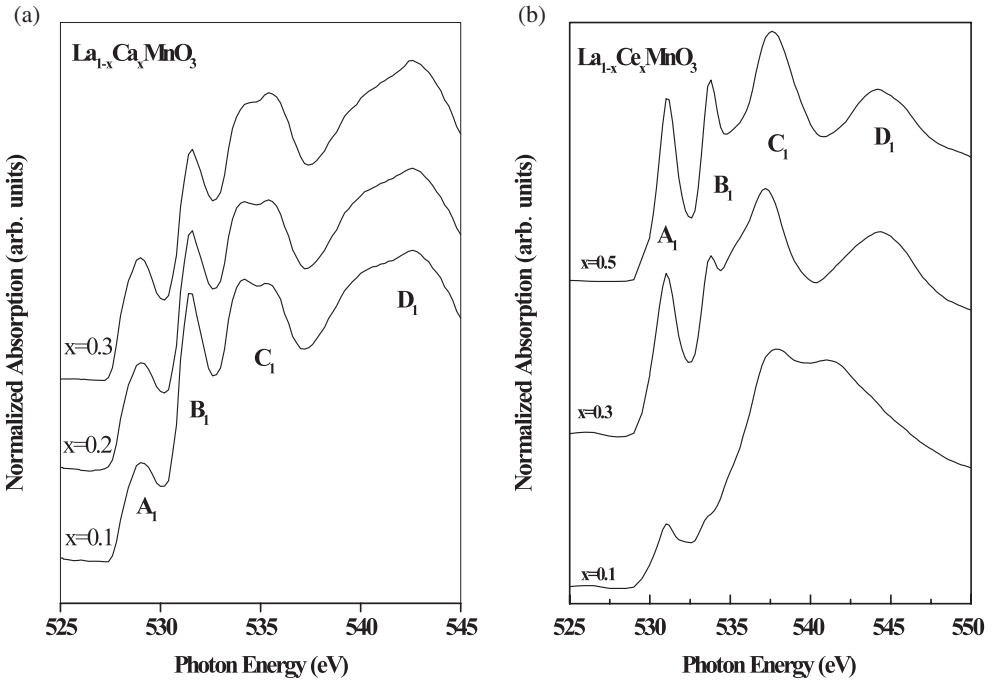

Figure 1. Normalized O K-edge XANES spectra of Ca- and Ce-doped $LaMnO_3$ manganites. Note that spectral features A_1 to D_1 are observable in all these samples.

the spectra are labelled as A_1 to D_1 in the energy range from 530 to 545 eV. All these features are commonly observed in perovskites [13] including titanates [14], nickelates [15] and also manganites [16, 17]. The leading features are attributable to O 2p–Mn 3d hybridization. The O 2p derived states lie predominantly in the valence band. The presence of O 2p derived states in the conduction band is due to couplings with cation orbitals. Thus, O K-edge XANES should depend sensitively on the local bonding arrangements of O ions. It is assumed that LM, with normal valence, $La^{3+}Mn^{3+}O_3^{2-}$, is an antiferromagnetic insulator. Mn^{3+} ions have four 3d electrons, and in the cubic environment the t_{2g} states lie lower in energy than the e_g ones [1–3]. The spins of the four 3d electrons are aligned by Hund's rule [2]. Accordingly, the features A_1 and B_1 were attributed to O 2p and Mn t_{2g} and e_g hybridized states, respectively, because the crystal field in the MnO_6 octahedron splits the Mn 3d band into t_{2g} and higher-energy e_g subbands. If one assigns the spectral features considering manganites as one of perovskites, the above procedure is consistent. However, if one considers reverse assignments, this leads to debatable issue [18, 19]. The O 2p derived states can be clearly seen in the normalized XANES spectra of the Ca-LM, Ce-LM, and LM compounds at the O K-edge, as shown in figure 2. In this figure the spectra of Mn_2O_3 and MnO compounds are also given for reference. The splitting between A_1 and B_1 is about 2.7 eV for the three Ca-LM, Ce-LM and LM spectra. Features A_1 and B_1 in the spectrum of Ca-LM are located at 529.9 and 532.6 eV with a chemical shift of ~ -0.5 eV relative to those of LM (shown in the figure by vertical lines). Both features A_1 and B_1 are much more prominent than those in the spectrum of LM. The enhancement of features A_1 and B_1 in the Ca-LM spectrum can be clearly seen in the difference spectra obtained by subtracting the spectrum of LM shown in the inset of figure 2, which has been referred to as an electron jump from the ligand [20]. The enhancement of features A_1 and

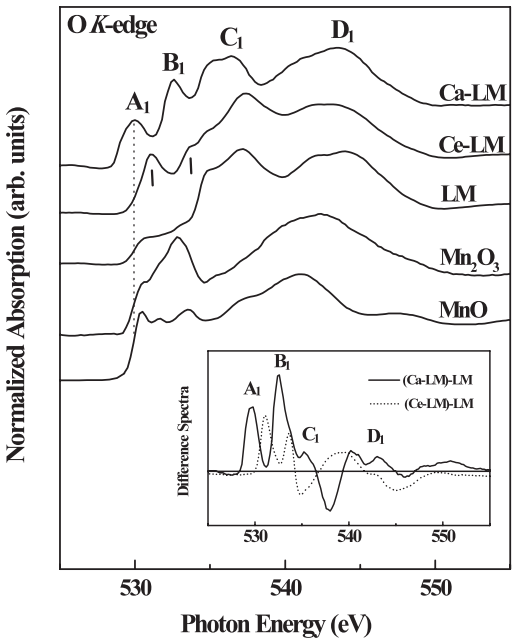

Figure 2. Normalized O K-edge XANES spectra of LM, Ca-LM and Ce-LM with reference compounds, MnO and Mn_2O_3. The dotted line indicates the shift in the energy position with respect to that of Ca-LM. The inset shows difference spectra obtained after subtracting the spectrum of LM, which reveals major differences between these manganites.

B_1 and the -0.5 eV chemical shift consistently show that the negative charge on the O ion is reduced. Features A_1 and B_1 in the spectrum of Ce-LM are located at 531.2 and 533.8 eV (also shown in the figure by vertical lines) with a chemical shift of $\sim$+1 eV relative to those of Ca-LM shows an increase of the negative charge on the O ion. This chemical shift has been recognized to be due to the more extended nature of the unoccupied O 2p derived states that are influenced by the reduced positive electrostatic potential at the Mn ions, which gain electrons from Ce dopants [20]. The Ca-LM and Ce-LM results are similar to those of the superconducting cuprates, in which the O K-edge XANES pre-edge peak of the electron-doped cuprate showed a +1 eV chemical shift from that of the hole-doped cuprate [21, 22]. Peak C_1 (534–538 eV) in the spectrum of Ca-LM was assigned to the La 5d–Ca 3d and O 2p hybridized states [16, 17]. The more prominent peak C_1 for Ce-LM than for Ca-LM was interpreted as an evidence of the involvement of La/Ce 5d/4f states [9, 16, 17, 21, 22]. It could be explained by the strong hybridization between the Ce(4f/5d) and Mn(3d) orbitals because Ca does not have near-edge f states. Based on the spectra of reference compounds, MnO and Mn_2O_3, the energy region between 538 and 548 eV, marked by D_1, was assigned to Mn 4sp–O 2p hybridized states [9, 16–18].

Figure 3(i) displays the normalized XANES spectra at the Mn K-edges of the Ca-LM and Ce-LM manganites along with the reference compounds Mn_2O_3 and MnO. The insets show the differences between the spectral shapes of the pre-edge and main features upon doping Ca and Ce ions. The pre-edge peak A_2 was assigned to the direct quadrupole transition from 1s to the empty Mn 3d states [23–25]. Inset (a) in the figure presents a magnified view of pre-edge A_2 after subtracting a Gaussian type background as shown by the dashed curve. This feature is relatively broad but noticeable in the spectrum of Ca-LM, indicating a significant probability

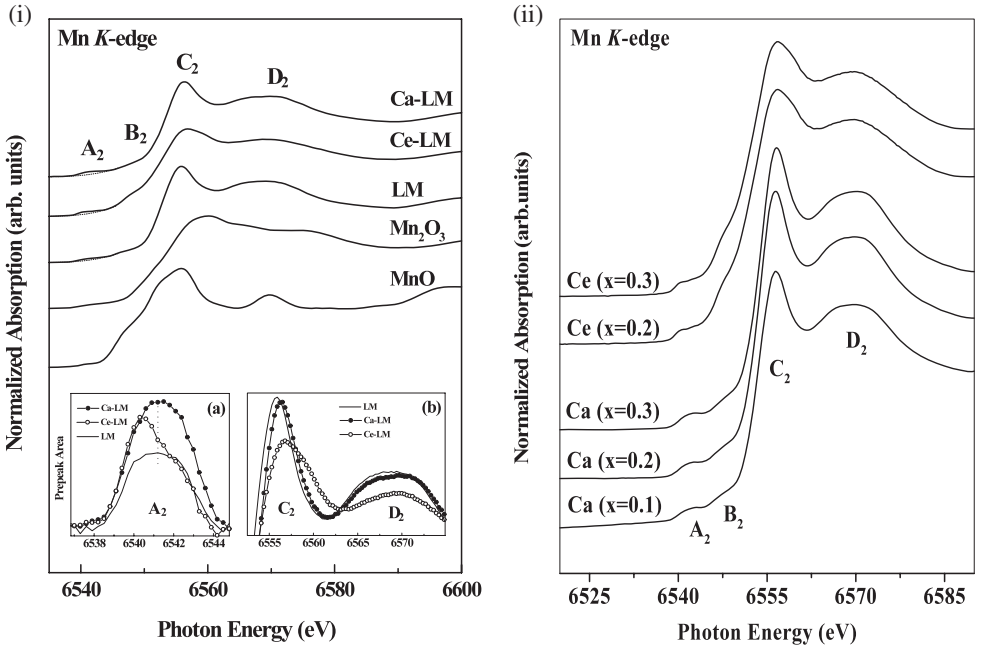

Figure 3. (i) Normalized Mn K-edge XANES spectra of manganites and reference compounds, MnO and Mn_2O_3, measured in fluorescence mode. The main spectral features are labelled as A_2 to D_2. Inset (a) is a magnified view of the pre-edge feature, A_2, after a Gaussian type background was subtracted. Notably, the centre of the pre-edge peak is shifted in the case of Ce-LM by $\sim$1 eV. Inset (b) plots the differences between features C_3 and D_3. (ii) Normalized Mn K-edge XANES spectra of some of the Ca- and Ce-doped manganites measured in fluorescence mode.

of transition from the Mn 1s electron to the empty t_{2g}- and e_g-O 2p hybridized states under the influence of the octahedral ligand field [23, 24]. The mixing of the Mn oxidation states has been argued to lead to a mixture of Mn 1s $\rightarrow$ 3d transition energies, which consequently broadens the pre-edge feature [23]. Beside differences in the intensities, the centres of the pre-edge feature A_2 in the Ce-LM (6540 eV) and Ca-LM (6541 eV) spectra differ by ~ -1 eV. This shows consistency in O and Mn K-edge measurements. The very shallow feature B_2 is only noticeable in the Ce-LM spectrum; it has been attributed to an increased p-character in the lowest empty Mn 3d-like electronic band [26]. Inset (b) in figure 3(i) shows the comparison of features C_2 and D_2 in the Ca-LM, Ce-LM and LM Mn K-edge spectra. Features C_2 and D_2 for Ca-LM are essentially the same as for LM except for a small shift to higher energy. The intensities of features C_2 and D_2 for Ce-LM, however, are substantially reduced relative to those for LM, which suggests that Ce doping enhances the occupation of Mn p orbitals. For the sake of completeness, XANES spectra of Mn K-edges at different concentrations of Ca and Ce are shown in figure 3(ii). These results suggest that the commonly accepted picture of a whole number charge state on Mn needs to be modified.

Figure 4 presents the normalized Mn $L_{3,2}$ XANES spectra of Ca-LM, Ce-LM, LM, MnO, and Mn_2O_3. These spectra are primarily due to the Mn 2p $\rightarrow$ 3d transition. The intensity of this line can be regarded as a measure of the total unoccupied Mn 3d states. The two broad multiple structures, L_3 and L_2, have been observed previously [27]. The L_3 region contains two spectral features, A_3 and B_3, which were assigned to Mn t_{2g} and e_g subbands, respectively [27]. The separation between A_3 and B_3 for Ca-LM, Ce-LM, and LM is essentially the same value,

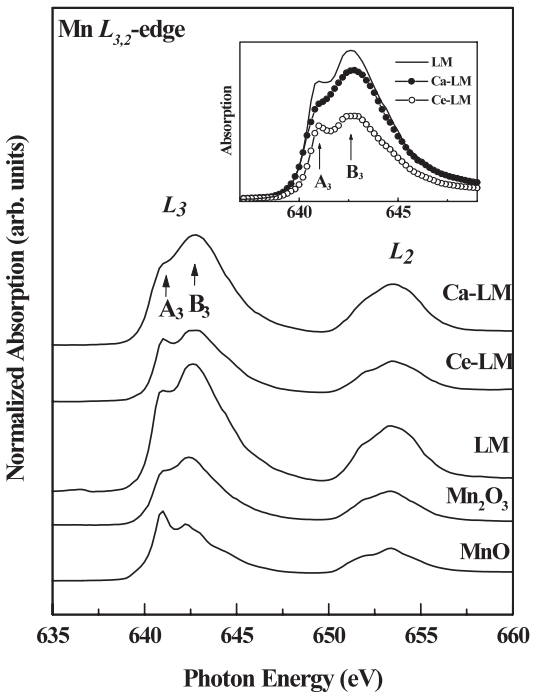

Figure 4. Normalized Mn $L_{3,2}$-edge XANES spectra of manganites and reference compounds, MnO and Mn_2O_3. The inset compares the intensities of the LM, Ca-LM and Ce-LM spectra.

1.7 eV. However, the A_3–B_3 separation of 1.7 eV is very different from the A_1–B_1 separation of 2.7 eV observed in the O K-edge XANES spectra. If we attribute features A_3 and B_3 to Mn t_{2g} and e_g states, we have a consistency problem. Thus, we need to re-interpret features A_3 and B_3. Mn ions in MnO have a 2+ charge state with the five 3d orbitals each filled by a majority-spin electron, so that features A_3 and B_3 can be attributed to minority-spin t_{2g} and e_g subbands, respectively. Here, the majority-spin is the spin of the electrons in the localized t_{2g} orbitals on the Mn ion. Later on we shall denote majority- and minority-spin as ↑spin and ↓spin, respectively. The larger intensity for A_3 than for B_3 is due to the fact that there are three t_{2g} orbitals and only two e_g orbitals. In Mn_2O_3, Mn ions have a 3+ oxidation state with the ↑spin e_g subband half-filled. Then the unoccupied part of the ↑spin e_g subband will contribute to the Mn $L_{3,2}$-edge spectrum. Thus, features A_3 and B_3 are contributed to not only from ↓spin t_{2g} and e_g subbands but also from ↑spin e_g subband. The Mn_2O_3 spectrum shows that feature B_3 has a larger intensity than feature A_3, which suggests that unoccupied ↑spin e_g states contribute more to feature B_3 than feature A_3. Mn ions in LM also have a 3+ charge state, so that its spectrum is similar to that of Mn_2O_3. Since features A_3 and B_3 contain contributions from the ↑spin e_g subband, the A_3–B_3 and A_1–B_1 separations do not need to be the same. Because of the Pauli exclusion principle, the ↑spin O 2p electrons shift away from the Mn ion, so that the O 2p-↑spin e_g and O 2p-↓spin e_g coupling strengths are different. The inset of figure 4 shows the intensity changes of features A_3 and B_3 in the spectra of Ca-LM and Ce-LM relative to those of LM. Since the ↓spin t_{2g} and e_g subbands are mostly unoccupied and are not significantly affected by Ca and Ce doping, the changes in features A_3 and B_3 are predominantly due to the changes in the filling of the ↑spin e_g subband. These changes reveal information about the averaged charge states of the Mn ions in Ca-LM and Ce-LM. The

intensities of features A_3 and B_3 in the Ce-LM spectrum are greatly reduced, which indicates that the number of unoccupied ↑spin e_g states decreases substantially and the charge state of the Mn ion is reduced. This result is compatible with the picture that Ce doping converts some Mn ions to Mn^{2+} and can be regarded as an electron doping. As for Ca-LM, the intensities of features A_3 and B_3 are also reduced, though to a lesser extent than those of Ce-LM as shown in the inset of figure 4. This result shows that the average number of ↑spin e_g electrons in Mn ions in Ca-LM is more than that in LM. Then the average (positive) charge state of the Mn ions in Ca-LM will be less than 3+, which is in contrast with the previous understanding that Ca doping converts a proportional number of Mn ions into Mn^{4+}. To reconcile our Mn $L_{3,2}$-edge XANES result for Ca-LM, Ca dopants have to create holes in some other orbitals. Figure 3(i) shows that the Ca-LM Mn K-edge spectrum is very similar to that of LM, so that Ca dopants do not create holes in Mn 4p orbitals. Then Ca dopants should create holes in the O 2p band. Indeed, as clearly shown in the inset of figure 2, the intensities of the O K-edge XANES spectrum for Ca-LM is greatly enhanced relative to that of LM, which is equivalent to the creation of holes in the O 2p derived states by Ca doping. It is interesting to note that from the inset of figure 2 our O K-edge XANES measurements also reveal the creation of holes in the O 2p derived states by Ce doping.

The DE model has been usually used to explain the normal state properties including the CMR phenomenon of manganites [1, 2, 4–6]. However, some recent studies showed that the DE mechanism alone could not explain all experimental results [1–3, 28]. Millis *et al* [29] argued against the DE model as the basic theory for the manganites, having shown, in particular, that its predictions for T_c and resistivity are an order of magnitude too high and too low, respectively. To explain the physical properties of the manganites it was proposed to include the lattice degrees of freedom [2, 28, 29].

The DE model is based on the assumptions that first the e_g orbitals are sufficiently delocalized, so that electrons occupying these orbitals are able to hop between adjacent Mn sites and give rise to metallic (strictly speaking semimetallic) property. Second, the e_g electrons are not too delocalized, so that their Hund's rule couplings with the ↑spin t_{2g} electrons are sufficiently strong to line up their spins with those of ↑spin t_{2g} electrons. Third, the ferromagnetic coupling integral between the spins of the e_g electrons is much larger than the antiferromagnetic coupling integral between t_{2g} electrons on adjacent Mn sites. These three assumptions lead to semimetallic and ferromagnetic properties of the material. Thus, within the DE model, the degree of delocalization of the e_g orbitals is crucial for semimetallic and ferromagnetic properties. Since an e_g electron cannot hop to another site with the two ↑spin e_g orbitals fully occupied, the hopping mechanism depends on the occupation of these e_g orbitals. The Mn ion in LM has been thought to have a 3+ charge state with 3 ↑spin t_{2g} and 1 ↑spin e_g electrons. Since LM is an antiferromagnetic insulator, if the DE model is applicable for manganites, the e_g orbitals have to be localized. However, our Mn $L_{3,2}$-edge XANES results as shown in figure 4 show that the degrees of delocalization of e_g orbitals in Ca-LM, Ce-LM, and LM are similar. Thus, the DE model cannot explain why LM is an antiferromagnetic insulator while Ca-LM and Ce-LM are ferromagnetic semimetals.

It has been argued that the occupation of e_g orbitals depends on the dopant and its concentration, and that these orbitals can be either localized or itinerant [3]. When La^{3+} ions are partially substituted by Ca^{2+} ions, a corresponding number of Mn ions become Mn^{4+} ions. The hopping of itinerant e_g electrons between spin-aligned Mn^{3+} and Mn^{4+} ions causes a DE interaction that results in an effective ferromagnetic interaction between Mn^{3+} and Mn^{4+} ions. Electron-doped manganites are obtained by doping Ce^{4+} ions, in which a similar DE interaction was argued to occur between Mn^{3+} and Mn^{2+} ions [5–7, 9, 10]. According to these arguments, mixed-valence Mn charge states are responsible for the correlation between magnetism and

conductivity [1, 6]. However, the Mn^{3+}/Mn^{4+} or Mn^{2+}/Mn^{3+} mixed-valent picture assumes that the Mn–O bond is 100% ionic, which is not supported by the electronegativity difference, 1.89, between Mn and O atoms (1.55 and 3.44 [30], respectively). This electronegativity difference is significantly less than that between an alkali/alkaline-earth element and oxygen. Thus, the Mn–O bond should contain a significant covalent component with partially occupied Mn 4s/4p orbitals. This mixed-valent picture also ignores the on-site electrostatic potential difference between Mn^{3+} and Mn^{4+} (or Mn^{3+} and Mn^{2+}) ions, which is about 8 eV without the screening effect. Ca-LM ($La_{0.7}Ca_{0.3}MnO_3$) is not a good conductor because it has a resistivity of the order of 10^{-2} Ω cm at the room temperature [31]. The screening effect is not sufficient to suppress the chemical shift due to the large on-site electrostatic potential difference between Mn^{3+} and Mn^{4+} ions. At room temperature, the CMR is in the paramagnetic state [9, 11]. Varma envisioned that in this state the spins of Mn^{3+} and Mn^{4+} ions are randomly oriented and fluctuate at frequencies related only to the temperature [32]. Since the orientation of the spin does not affect the on-site electrostatic potential, both room-temperature photoemission and XANES spectra of the CMR should reflect the large chemical shift and show two distinctive sets of Mn 3d-derived features. However, the extra set of Mn 3d-derived features are absent in the present XANES spectra and those obtained previously [12, 18] and the photoemission spectra of Park *et al* [12]. The Mn $L_{3,2}$-edge results also do not show any Ce and Ca dopant-induced localization to delocalization transition of the e_g orbitals.

In the DE model, the oxygen ion is in a closed shell (O^{2-}) connecting two neighbouring Mn ions and permitting the hopping of the e_g electron between the Mn ions [28]. The above XANES results indicate that the Ca and Ce doping essentially creates holes at the ligand (p-hole) rather than in Mn ions (d-hole). It may be noted that the p-hole picture does not appear in the DE model since antiferromagnetic coupling between the Mn local spins and the p-holes is weak compared with the large oxygen bandwidth [2]. The above discussions clearly indicate the need for new theoretical models other than DE-based models to understand the properties of manganites.

4. Conclusions

In conclusion, spectroscopic data obtained using XANES measurements at the O K-, Mn K-, and Mn $L_{3,2}$-edges for the hole-doped $La_{0.7}Ca_{0.3}MnO_3$, electron-doped $La_{0.7}Ce_{0.3}MnO_3$ and undoped $LaMnO_3$ manganites are compared in detail. The Mn $L_{3,2}$- and K-edge results show that Ce dopants donate electrons to increase the occupation of both Mn ↑spin e_g and 4p orbitals on some Mn ions. However, the O K-edge results show that Ce doping induces holes in O 2p derived states. From both O K- and Mn K-edge results we find instead that the holes created by Ca dopants are in the O 2p derived states. Since our Mn $L_{3,2}$-edge results do not show any evidence of the creation of the Mn^{4+} state by Ca doping and the localization of ↑spin e_g orbitals, the DE model may not be suitable for the explanation of why $LaMnO_3$ is an antiferromagnetic insulator and hole- and electron-doped manganites become ferromagnetic semimetals.

Acknowledgments

The authors are grateful to Dr P A Joy, National Chemical Laboratory, Pune, for providing Ca-doped samples. KA and SM thank the director of the Nuclear Science Center for granting them leave and encouragement. KA and WFP would like to thank the National Science Council of the Republic of China, for financially supporting this research under Contract no. NSC91-2112-M-032-015. The SRRC staff is also appreciated for their technical support.

References

[1] For review and references: Tokura Y (ed) 2000 *Colossal Magnetoresistive Oxides* (The Netherlands: Gordon and Breach)
Coey J M D, Viret M and von Molnar S 1999 *Adv. Phys.* **48** 167
[2] Edwards D M 2002 *Adv. Phys.* **51** 1259
[3] Dagotto E, Hottta T and Moreo A 2001 *Phys. Rep.* **344** 1
[4] Renner Ch, Aeppli G, Kim B-G, Soh Y-A and Cheng S-W 2002 *Nature* **416** 518
[5] Das S and Mandal P 1997 *Indian J. Phys.* A **71** 231
[6] Gebhardt J R, Roy S and Ali N 1999 *J. Appl. Phys.* **85** 5390
[7] Kang J-S, Kim Y J, Lee W B, Olson C G and Min B I 2001 *J. Phys.: Condens. Matter* **13** 3779
[8] Stöhr J 1992 *NEXAFS Spectroscopy* (Berlin: Springer)
[9] Asokan K *et al* 2002 *Surf. Rev. Lett.* **9** 1053
[10] Mitra C *et al* 2003 *Phys. Rev.* B **67** 092404 and reference therein
[11] Anil Kumar P S, Joy P A and Date S K 1998 *J. Phys.: Condens. Matter* **10** L269
Husain S, Choudhary R J, Kumar R, Patil S I and Srivastava J P 2002 *Pramana* **58** 1045
[12] Park J-H, Kimura T and Tokura Y 1998 *Phys. Rev.* B **58** R13330
[13] van Aken P A, Liebscher B and Styrsa V J 1998 *Phys. Chem. Minerals* **25** 494
[14] Asokan K *et al* 2001 *J. Phys.: Condens. Matter* **13** 11087
[15] Sarma D D *et al* 1994 *Phys. Rev.* B **49** 14238
[16] Abbate M, Cruz D Z N, Zampieri G, Briatico J, Causa M T, Tovar M, Caneiro A, Alascio B and Morikawa E 1997 *Solid State Commun.* **103** 9
[17] Abbate M *et al* 1992 *Phys. Rev.* B **46** 4511
[18] Park J-H, Chen C T, Cheong S-W, Bao W, Meigs G, Chakarian V and Idzerda Y U 1996 *Phys. Rev. Lett.* **76** 4215
[19] Solovyev V *et al* 2003 *Preprint* cond-mat/0303668
Hozoi L 2003 Localized states in transition metal oxides *PhD Thesis* Rijksuniversiteit Groningen (RUG), The Netherlands
[20] Glaser T, Hedman B, Hodgson K O and Solomon E I 2000 *Acc. Chem. Res.* **33** 859
[21] Krol A, Lin C S, Ming Z H, Sher C J, Kao Y H, Lin C L, Qiu S L, Chen J, Tranquada J M, Strongin M, Smith G C, Tao Y K, Meng R L, Hor P H, Chu C W, Gao G and Crow J W 1990 *Phys. Rev.* B **42** 4763
[22] Pellegrin E, Nucker N, Fink J, Molodtsov S L, Gutierrez A, Navas E, Strebel O, Hu Z, Domke M, Kaindl G, Uchida S, Nakamura Y, Markl J, Klauda M, Saemann-Ischenko G, Krol A, Peng J L, Li Z Y and Greene R L 1993 *Phys. Rev.* B **47** 3354
[23] Ignatov A Y, Ali N and Khalid S 2001 *Phys. Rev.* B **64** 14413 and references therein
[24] Bridges F, Booth C H, Kwei G H, Neumeiere J J and Sawatzky G A 2000 *Phys. Rev.* B **61** R9237
Zeng Z, Greenblatt M and Croft M 2001 *Phys. Rev.* B **63** 224410
[25] Croft M, Sills D, Greenblatt M, Lee C, Cheong S-W, Ramanujachary K V and Tran D 1997 *Phys. Rev.* B **55** 8726
[26] Franke R, Rothe J, Becker R, Pollmann J, Hormes J, Bonnemann H, Brijoux W and Kopper R 1998 *Adv. Mater.* **10** 126
[27] Liu R S, Jang L Y, Chen J M, Wu J B, Liu R G, Lin J G and Huang C Y 1998 *Solid State Commun.* **105** 605
[28] Izyumov Yu A and Skryabin Yu N 2001 *Phys.—Usp.* **44** 109
[29] Millis A J, Littlewood P B and Shraiman B I 1995 *Phys. Rev. Lett.* **74** 5144
[30] *Table of Periodic Properties of the Elements* 1980 (Skokie, IL: Sargent-Welch Scientific Company)
[31] Lu C J, Wang Z L, Kwon C and Jia Q X 2000 *J. Appl. Phys.* **88** 4032
[32] Varma C M 1996 *Phys. Rev.* B **54** 7328